J|A|C|S ARTICLES

Published on Web 09/22/2009

Dehydrocoupling Reactions of Borane−Secondary and −Primary Amine Adducts Catalyzed by Group-6 Carbonyl Complexes: Formation of Aminoboranes and Borazines

Yasuro Kawano,*,† Mikio Uruichi,‡,⊥ Mamoru Shimoi,*,† Seitaro Taki,† Takayuki Kawaguchi,† Taeko Kakizawa,†,¶ and Hiroshi Ogino‡,§

Department of Basic Science, Graduate School of Arts and Sciences, University of Tokyo, Meguro-ku, Tokyo 153-8902, Japan, Department of Chemistry, Graduate School of Science, Tohoku University, Sendai 980-8578, Japan, and The Open University of Japan, Wakaba 2-11, Mihama-ku, Chiba 261-8586, Japan

Received June 16, 2009; E-mail: ckawano1@mail.ecc.u-tokyo.ac.jp; cshimoi@mail.ecc.u-tokyo.ac.jp

Abstract: Photoirradiation of a solution of $BH_3{\cdot}NHR_2$ (**1a:** R = Me, **1b:** R = $1/2C_4H_8$, **1c:** R = $1/2C_5H_{10}$, **1f:** R = Et) containing a catalytic amount of a group-6 metal carbonyl complex, $[M(CO)_6]$ (M = Cr, Mo, W), led to dehydrogenative B−N covalent bond formation to produce aminoborane dimers, $[BH_2NR_2]_2$ (**2a**−**c**, **f**), in high yield. During these reactions a borane σ complex, $[M(CO)_5(\eta^1\text{-}BH_3{\cdot}NHR_2)]$ (**3**), was detected by NMR spectroscopy. Similar catalytic dehydrogenation of bulkier amineboranes, $BH_3{\cdot}NH^iPr_2$ (**1d**) and $BH_3{\cdot}NHCy_2$ (**1e**, Cy = *cyclo*-C_6H_{11}), afforded monomeric products $BH_2{=}NR_2$ (**4d**, **e**). The reaction mechanism of the dehydrocoupling was investigated by DFT calculations. On the basis of the computational study, we propose that the catalytic dehydrogenation reactions proceed via an intramolecular pathway and that the active catalyst is $[Cr(CO)_4]$. The reaction follows a stepwise mechanism involving NH and BH activation. Dehydrocoupling of borane−primary amine adducts $BH_3{\cdot}NH_2R$ (**1g:** R = Me, **1h:** R = Et, **1i:** R = ^{t}Bu) gave borazine derivatives $[BHNR]_3$ (**5g**−**i**).

Introduction

Transition metal-catalyzed dehydrocoupling reactions of p-block element hydrides attract much attention for both academic and practical reasons, and provide efficient synthetic routes to new inorganic oligomers and polymers.[1] This methodology was first applied to the synthesis of polysilane polymers,[2] and to date, has been extended to oligomers and polymers containing various p-block elements in the backbone.[3] In the past few years, Manners and co-workers actively studied Rh-, Ru-, and Ti-catalyzed dehydrocoupling reactions of amineboranes and phosphineboranes to produce aminoborane and phosphinoborane oligomers and polymers.[4,5]

Furthermore, this research area is currently expanding toward the utilization of amineboranes as hydrogen storage materials.[6−12] Since simple amineboranes (in particular $BH_3{\cdot}NH_3$) have a large hydrogen content and release H_2 through the dehydrocoupling reaction, they are promising candidates for hydrogen storage materials. Thus, investigation of catalytic dehydrocoupling

† University of Tokyo.
‡ Tohoku University.
§ The Open University of Japan.
⊥ Present address: Institute of Molecular Science, 38 Nishigo-Naka, Myodaiji, Okazaki 444-8585, Japan.
¶ Present address: Laboratory of Proteomic Sciences, 21st Century COE Program, Kyoto Pharmaceutical University, Yamashina-ku, Kyoto 607-8412, Japan.

(1) (a) Gauvin, F.; Harrod, J. F.; Woo, H. G. *Adv. Organomet. Chem.* **1998**, *42*, 363. (b) Clark, T. J.; Lee, K.; Manners, I. *Chem.—Eur. J.* **2006**, *12*, 8634. (c) Hamilton, C. W.; Baker, R. T.; Staubitzc, A.; Manners, I. *Chem. Soc. Rev.* **2009**, *38*, 279.
(2) Corey, J. Y. *Adv. Organomet. Chem.* **2004**, *51*, 1.
(3) For example: (a) Aitken, C.; Harrod, J. F.; Malek, A.; Samuel, E. *J. Organomet. Chem.* **1988**, *349*, 285. (b) Choi, N.; Tanaka, M. *J. Organomet. Chem.* **1998**, *564*, 81. (c) Neale, N. R.; Tilley, T. D. *J. Am. Chem. Soc.* **2005**, *127*, 14745. (d) Fermin, M. C.; Stephan, D. W. *J. Am. Chem. Soc.* **1995**, *117*, 12645. (e) Böhm, V. P. W.; Brookhart, M. *Angew. Chem., Int. Ed.* **2001**, *40*, 4694. (f) Waterman, R.; Tilley, T. D. *Angew. Chem., Int. Ed.* **2006**, *45*, 2926.
(4) Jaska, C. A.; Manners, I. In *Inorganic Chemistry in Focus II*; Meyer, G., Naumann, D., Wesemann, L., Eds.; Wiley-VCH: Weinheim, 2005; pp 53−64.
(5) Staubitz, A.; Soto, A. P.; Manners, I. *Angew. Chem., Int. Ed.* **2008**, *47*, 6212.
(6) Denney, M. C.; Pons, V.; Hebden, T. J.; Heinekey, D. M.; Goldberg, K. I. *J. Am. Chem. Soc.* **2006**, *128*, 12048.
(7) Keaton, R. J.; Blacquiere, J. M.; Baker, R. T. *J. Am. Chem. Soc.* **2007**, *129*, 1844.
(8) Clark, T. J.; Whittell, G. R.; Manners, I. *Inorg. Chem.* **2007**, *46*, 7522.
(9) Blaquiere, N.; Diallo-Garcia, S.; Gorelsky, S. I.; Black, D. A.; Fagnou, K. *J. Am. Chem. Soc.* **2008**, *130*, 14034.
(10) Käss, M.; Friedrich, A.; Drees, M.; Schneider, S. *Angew. Chem., Int. Ed.* **2009**, *48*, 905.
(11) Reviews of chemical hydrogen storage: (a) Grochala, W.; Peter, P.; Edwards, P. P. *Chem. Rev* **2004**, *104*, 1283. (b) Marder, T. B. *Angew. Chem., Int. Ed.* **2007**, *46*, 8116.
(12) Thermolytic dehydrogenation of $BH_3{\cdot}NH_3$ in ionic liquids: (a) Bluhm, M. E.; Bradley, M. G.; Butterrick, R., III.; Kusari, U.; Sneddon, L. G. *J. Am. Chem. Soc.* **2006**, *128*, 7748. Hydrogen release from $BH_3{\cdot}NH_3$ through the action of acids: (b) Stephens, F. H.; Baker, R. T.; Matus, M. H.; Grant, D. J.; Dixon, D. A. *Angew. Chem., Int. Ed.* **2007**, *46*, 746. Dehydrogenation of $BH_3{\cdot}NH_3$ on mesoporous materials: (c) Gutowska, A.; Li, L.; Shin, Y.; Wang, C. M.; Li, X. S.; Linehan, J. C.; Smith, R. S.; Kay, B. D.; Schmid, B.; Shaw, W.; Gutowski, M.; Autrey, T. *Angew. Chem., Int. Ed.* **2005**, *44*, 3578.

 10.1021/ja904918u CCC: $40.75

Chart 1

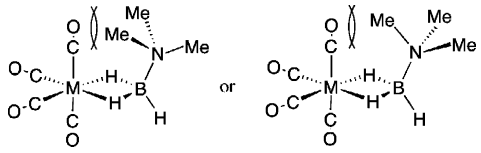

reactions has influenced the development of new energy systems such as fuel cells.

We previously reported the synthesis and properties of a series of borane σ complexes, $[M(CO)_5(\eta^1\text{-}BH_3\cdot L)]$ (M = Cr, Mo, W; L = NMe_3, PMe_3, PPh_3).[13] In these compounds, the borane ligand coordinates to the central metal through a B−H−M three-center two-electron bond and is quite labile. The syntheses of these compounds were accomplished by the photolysis of $[M(CO)_6]$ in the presence of neutral borane adducts $BH_3\cdot L$, where L is a tertiary amine or phosphine (eq 1).

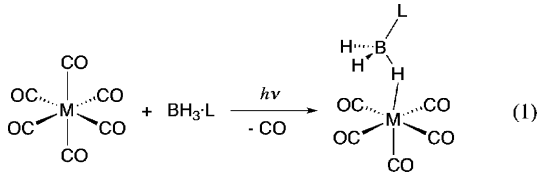

(1)

M = Cr, Mo, W; L = NMe_3, PMe_3, PPh_3

Interestingly, prolonged photoirradiation did not lead to further dissociation of CO followed by the formation of bidentate derivatives, $[M(CO)_4(\eta^2\text{-}BH_3\cdot L)]$. This result was somewhat surprising because the closely related borohydrides, $[M(CO)_4(\eta^2\text{-}BH_4)]^-$, included a bidentate BH_4^- ligand.[14−16] It is also in a contrast to the behavior of monodentate diborane(4) complexes, $[M(CO)_5(\eta^1\text{-}B_2H_4\cdot 2PMe_3)]$, which are converted to the bidentate derivatives $[M(CO)_4(\eta^2\text{-}B_2H_4\cdot 2PMe_3)]$ through dissociation of a carbonyl ligand induced by photoirradiation or heating.[17] For such a difference between the coordination modes of $BH_3\cdot L$ and BH_4^- (or $B_2H_4\cdot 2PMe_3$), there are two possible rationales:

(1) Owing to the lability of the borane−metal linkage, further irradiation of the complex predominantly causes borane dissociation rather than CO expulsion.

(2) Steric interaction between the base on boron and a carbonyl ligand prevents the formation of the bidentate species. Indeed, in the hypothetical bidentate complex $[Cr(CO)_4(\eta^2\text{-}BH_3\cdot NMe_3)]$, nonbonding distances between the carbonyl oxygen and methyl carbon atoms were calculated to be shorter than the sum of the van der Waals radii of oxygen and a methyl group (Chart 1).

If the latter rationale is correct, the use of sterically less demanding boranes might produce the bidentate species.

On the basis of such a hypothesis, we attempted the photoreaction of $[Cr(CO)_6]$ with borane−dimethylamine adduct, $BH_3\cdot NHMe_2$ (**1a**). However, this trial did not afford the bidentate complex, but resulted in dehydrocoupling (formation of a B−N covalent bond) of the amineborane to produce a cyclic aminoborane dimer, $[BH_2NMe_2]_2$ (**2a**). During the reaction, a borane σ complex $[Cr(CO)_5(\eta^1\text{-}BH_3\cdot NHMe_2)]$ (**3a**) was detected. We then found that the dehydrocoupling proceeded even with use of a catalytic amount of $[M(CO)_6]$ and applied this reaction to various borane−amine adducts.

In this paper, we report details of the dehydrocoupling reactions of borane−amine adducts, including a mechanistic study conducted by DFT calculations. This catalytic reaction is important as a synthetic route to aminoboranes and borazines, which can be utilized as precursors of BN ceramics,[18] because forcing conditions are not required here. A part of this work has been published already.[19] Formation of **3a** and its decomposition leading to **2a** have also been reported by Heinekey and co-workers.[20] Other amineborane derivatives are mentioned in their report.

Results and Discussion

Dehydrocoupling of Borane−Secondary Amine Adducts Catalyzed by $[M(CO)_6]$. A THF solution of $BH_3\cdot NHMe_2$ (**1a**) and a catalytic amount (0.6 mol %) of $[Cr(CO)_6]$ was photolyzed using a 450 W medium pressure Hg lamp for 1 h, after which time the solution was stirred in the dark for 1 day. During the photolysis, a gas was vigorously evolved, and a pale yellow solution was produced. The gas evolution continued even after the irradiation was terminated. However, it ceased after a day of the reaction, and the yellow color disappeared to leave a pale green suspension. From the resulting mixture, a cyclic aminoborane dimer $[BH_2NMe_2]_2$ (**2a**)[21] was isolated by sublimation in 69% yield (eq 2). Because of the formation of the boron−nitrogen covalent bond, this reaction is described as a chromium-catalyzed dehydrogenative B−N coupling of **1a**.

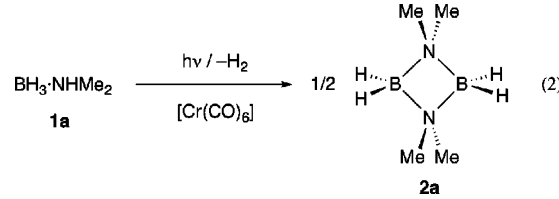

(2)

Table 1 summarizes the results of photolysis of various borane−secondary amine adducts in the presence of catalytic amounts of $[M(CO)_6]$. Pyrrolidineborane (**1b**) and piperidineborane (**1c**) underwent dehydrogenation like **1a** to give $[BH_2N(CH_2)_4]_2$ (**2b**) and $[BH_2N(CH_2)_5]_2$ (**2c**),[22] respectively, in high yields. At the early stage of these reactions, borane σ complexes $[Cr(CO)_5(\eta^1\text{-}BH_3\cdot NHR_2)]$ (**3a**: R = Me, **3b**: R = $1/2C_4H_8$, **3c**: R = $1/2C_5H_{10}$) were detected by ^1H and ^{11}B NMR spectroscopy. Details of compound **3** will be described in a later

(13) Shimoi, M.; Nagai, S.; Ichikawa, M.; Kawano, Y.; Katoh, K.; Uruichi, M.; Ogino, H. *J. Am. Chem. Soc.* **1999**, *121*, 11704.

(14) Kirtley, S. W.; Andrews, M. A.; Bau, R.; Grynkewich, G. W.; Marks, T. J.; Tipton, D. L.; Whittlesey, B. R. *J. Am. Chem. Soc.* **1977**, *99*, 7154.

(15) Darensbourg, M. Y.; Bau, R.; Marks, M. W.; Burch, R. R., Jr.; Deaton, J. C.; Slater, S. *J. Am. Chem. Soc.* **1982**, *104*, 6961.

(16) Wei, C.-Y.; Marks, M. W.; Bau, R.; Kirtley, S. W.; Bisson, D. E.; Henderson, M. E.; Koetzle, T. F. *Inorg. Chem.* **1982**, *21*, 2556.

(17) (a) Katoh, K.; Shimoi, M.; Ogino, H. *Inorg. Chem.* **1992**, *31*, 670. (b) Shimoi, M.; Katoh, K.; Ogino, H. *J. Chem. Soc., Chem. Commun.* **1990**, 811.

(18) For example, Toury, B.; Miele, P.; Cornu, D.; Vincent, H.; Bouix, J. *Adv. Funct. Mater* **2002**, *12*, 228.

(19) Shimoi, M.; Katoh, K.; Uruichi, M.; Nagai, S.; Ogino, H. *Current Topics in the Chemistry of Boron*; Kabalka, G. W., Ed.; The Royal Society of Chemistry: London; 1994, pp 293−296.

(20) Pons, V.; Denney, M. C.; Goldberg, K. I.; Heinekey, D. M. *Prepr. Symp. Am. Chem. Soc. Div. Fuel Chem.* **2005**, *50*, 51.

(21) (a) Burg, A. B.; Randolph, C. L., Jr. *J. Am. Chem. Soc.* **1949**, *71*, 3451. (b) Haubold, W.; Schaeffer, R. *Chem. Ber.* **1971**, *104*, 513. (c) Nöth, H.; Vahrenkamp, H. *Chem. Ber.* **1967**, *100*, 3353.

(22) (a) Storr, A.; Thomas, B. S.; Penland, A. D. *J. Chem. Soc., Dalton Trans.* **1972**, 326. (b) Nöth, H.; Wrackmeyer, B. *Chem. Ber.* **1974**, *107*, 3070. (c) Pasumansky, L.; Haddenham, D.; Clary, J. W.; Fisher, G. B.; Goralski, C. T.; Singaram, B. *J. Org. Chem.* **2008**, *73*, 1898.

Table 1. Group-6 Metal-Catalyzed Dehydrogenation Reaction of Borane−Secondary Amine Adducts

borane	catalyst(5 mol %)	condition[a]	conversion/ %	yield of products[b]/%				
				$[BH_2NR_2]_2$(**2**)	$BH_2{=}NR_2$(**4**)	$[BH_2NR_2]_3$ (**6**)	$BH(NR_2)_2$ (**7**)	$B_2H_5(\mu\text{-}NR_2)$(**8**)
$BH_3{\cdot}NHMe_2$ (**1a**)	$[Cr(CO)_6]$	*hν* 1 h	95	90	0.2	2	2	6
	$[Cr(CO)_6]$	*hν* 5 min + RT 1 d[c]	100	95	0.2	0.3	1	3
	$[Mo(CO)_6]$	*hν* 1 h	90	94	0.7	2	1	2
	$[W(CO)_6]$	*hν* 1 h	84	95	2	0.6	0.4	1
	$[Cr(CO)_5(thf)]$	RT 90 min[d]	97	94	0.1	2	0.1	3
	$[Cr(CO)_5(\eta^1\text{-}BH_3{\cdot}NMe_3)]$	RT 60 min[d]	97	93	0.2	2	0.1	3
$BH_3{\cdot}NH(CH_2)_4$ (**1b**)	$[Cr(CO)_6]$	*hν* 5 min + RT 1 d[c]	98	97	-	-	0.8	-
$BH_3{\cdot}NH(CH_2)_5$ (**1c**)	$[Cr(CO)_6]$	*hν* 1 h	100	93	2.5	2	2	-
	$[W(CO)_6]$	*hν* 1 h	71	88	8	-	2	-
	$[W(CO)_6]$	*hν* 1 h + RT 1 d[c]	100	98	0.3	-	1	-
$BH_3{\cdot}NH^iPr_2$ (**1d**)	$[Cr(CO)_6]$	*hν* 1 h	24	-	71	-	6	-
	$[W(CO)_6]$	*hν* 1 h	12	-	79	-	11	-
$BH_3{\cdot}NHCy_2$ (**1e**)	$[Cr(CO)_6]$	*hν* 8 h	61	-	78	-	12	10
$BH_3{\cdot}NHEt_2$ (**1f**)	$[Cr(CO)_6]$	*hν* 1 h	87	53	17	-	11	-
	$[W(CO)_6]$	*hν* 1 h	68	5	72	-	17	-
	$[W(CO)_6]$	*hν* 1 h + RT 1 d[c]	100	57	14	-	14	9

[a] Photolyses were carried out at 8 °C using a 450 W medium pressure Hg lamp. [b] The yield to the conversion, judged by NMR. [c] After the photolysis, the sample was allowed to stand in the dark at RT. [d] In the dark.

section. Some minor products $[BH_2NR_2]_3$ (**6**),[23] $BH(NR_2)_2$ (**7**),[24] and $B_2H_5(\mu\text{-}NR_2)$ (**8**)[25] were also detected after the reaction. Dehydrogenation of **1a** and **1c** took place even when $[W(CO)_6]$ was employed as a catalyst; however, the tungsten-catalyzed reaction was slower than the chromium-mediated cases. Molybdenum carbonyl also catalyzed the dehydrocoupling of **1a**. It should be noted that the dehydrocoupling proceeds through short-period photochemical initiation and subsequent thermal reaction in the dark. In addition, the dehydrocoupling of **1a** was catalyzed even by $[Cr(CO)_5(thf)]$ and $[Cr(CO)_5(\eta^1\text{-}BH_3{\cdot}NMe_3)]$. These observations indicate that $[Cr(CO)_5]$ acts as the active catalyst or its precursor and that the dehydrocoupling proceeds thermally after the active species is generated in the reaction system.

Bulky amineboranes, $BH_3{\cdot}NH^iPr_2$ (**1d**) and $BH_3{\cdot}NHCy_2$ (**1e**), showed different reactivity. Their dehydrogenation was much slower than that of **a**−**c**. In the chromium-catalyzed reaction, the conversion of **1d** was 24% after 1 h of photolysis. More importantly, the major products were monomeric aminoboranes $BH_2{=}NR_2$ (**4d**: R = ^{i}Pr, **4e**: R = Cy),[22c] and no formation of the cyclic dimer was observed (eq 3). These results are parallel to Manners' Rh and Ru-catalyzed systems.[26,27]

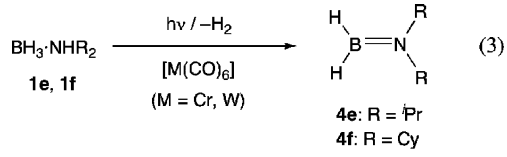

(3)

The behavior of $BH_3{\cdot}NHEt_2$ (**1f**) is of interest. In the tungsten-catalyzed reaction, monomeric $BH_2{=}NEt_2$ (**4f**)[21c,22c] was observed after 1 h of photolysis as the main component. However, when the reaction mixture was allowed to stand for 1 day, **4f** decreased dramatically and the dimer **2f** alternatively became the major product. Thus, in this case, the initial formation of the monomeric product and its subsequent dimerization were apparently observed.

Metal-Catalyzed Dehydrocoupling of Borane−Primary Amine Adducts. Group-6 metal-catalyzed dehydrocoupling can also be applied to borane−primary amine adducts, $BH_3{\cdot}NH_2Me$ (**1g**) and $BH_3{\cdot}NH_2Et$ (**1h**). In these cases, however, further dehydrogenation proceeded to yield borazine derivatives **5g** and **5h** in good yields (eq 4).[23c,d,28] When the reaction of **1g** was monitored in benzene-d_6, it was apparent that the precursor was consumed within 1 h of photolysis as evidenced by ^{11}B NMR. At this stage, broad resonances appeared at 0 to −10 ppm in the ^{11}B NMR spectrum of the reaction mixture, and a considerable amount of a white viscous material precipitated. This is assignable to intermediates in the borazine formation process, a mixture of aminoborane oligomers $[BH_2NHMe]_n$. Further irradiation and subsequent dark reaction at RT led to the disappearance of the precipitate and formation of borazine **5g** in good yield. The ethyl derivative **1h** dehydrocoupled similarly to yield **5h**. Unlike the methyl derivative, the intermediate $[BH_2NHEt]_n$ was considerably soluble in benzene-d_6, and showed intense signals at −5 to −10 ppm in the ^{11}B NMR spectrum. Thus, **1g** and **1h** undergo catalytic dehydrogenation to produce oligomeric aminoboranes, which are then converted to borazines **5**. Recently, Ir-catalyzed formation of polymeric aminoboranes, $[BH_2NHR]_n$ (R = H, Me), was reported by the Manners and Heinekey groups.[5,29]

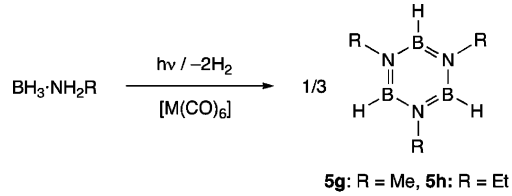

(4)

Table 2 summarizes the results of dehydrogenation of various primary amine adducts. The formation of **5g** was also catalyzed

(23) (a) Narula, C. K.; Janik, J. F.; Duesler, E. N.; Paine, R. T.; Schaeffer, R. *Inorg. Chem.* **1986**, *25*, 3346. (b) Campbell, G. W.; Johnson, L. *J. Am. Chem. Soc.* **1959**, *81*, 3800. (c) Bissot, T. C.; Parry, R. W. *J. Am. Chem. Soc.* **1955**, *77*, 3481. (d) Nöth, H.; Wrackmeyer, B. *Chem. Ber.* **1981**, *114*, 1150.

(24) (a) Burg, A. B.; Randolph, C. L., Jr. *J. Am. Chem. Soc.* **1951**, *73*, 953. (b) Ashby, E. C.; Kovar, R. A.; Culbertson, R. *Inorg. Chem.* **1971**, *10*, 900.

(25) Phillips, W. D.; Miller, H. C.; Muetterties, E. L. *J. Am. Chem. Soc.* **1959**, *81*, 4496.

(26) (a) Jaska, C. A.; Temple, K.; Lough, A. J.; Manners, I. *Chem. Commun.* **2001**, 962. (b) Jaska, C. A.; Temple, K.; Lough, A. J.; Manners, I. *J. Am. Chem. Soc.* **2003**, *125*, 9424.

(27) Sloan, M. E.; Clark, T. J.; Manners, I. *Inorg. Chem.* **2009**, *48*, 2429.

(28) (a) Hough, W. V.; Schaeffer, G. W.; Dzurus, M.; Stewart, A. C. *J. Am. Chem. Soc.* **1955**, *77*, 864. (b) Ashby, E. C.; Kovar, R. A. *Inorg. Chem.* **1971**, *10*, 1524.

Table 2. Metal-Catalyzed Dehydrogenation Reaction of Borane−Primary Amine Adducts

				yield of products[b]/%				
borane	catalyst (5 mol %)	condition[a]	conversion/ %	$[BHNR]_3$(**5**)	$[BH_2NHR]_n$	BH_2=NHR (**4**)	$BH(NHR)_2$ (**7**)	$B_2H_5(\mu$-NHR) (**8**)
$BH_3\cdot NH_2Me$(**1g**)	$[Cr(CO)_6]$	hν 1 h	98	<30	>30	−	trace	12
		hν 8 h + RT 1 d[c]	99	80	10	−	trace	3
	$[Mo(CO)_6]$	hν 1 h	50	<10	>40	−	trace	20
		hν 8 h + RT 1 d[c]	99	70	10	−	trace	5
	$[W(CO)_6]$	hν 1 h	54	trace	>40	−	−	5
		hν 8 h + RT 1 d[c]	98	35	35	−	trace	9
$BH_3\cdot NH_2Et$ (**1h**)	$[Cr(CO)_6]$	hν 1 h	80	22	55	0.2	trace	15
		hν 8 h + RT 1 d[c]	100	75	20	−	−	2
	$[W(CO)_6]$	hν 8 h + RT 1 d[c]	38	2		5	20	68
$BH_3\cdot NH_2{}^t$Bu (**1i**)	$[Cr(CO)_6]$	hν 8 h + RT 1 d[c]	99	19		−	10	55
	$[W(CO)_6]$	hν 8 h + RT 1 d[c]	40			5	18	68

[a] Photolyses were carried out at 8 °C using a 450 W medium pressure Hg lamp. [b] The yield to the conversion, judged by NMR. [c] After the photolysis, the sample was allowed to stand in the dark at RT.

by $[Mo(CO)_6]$ and $[W(CO)_6]$. Bulky $[BHN^tBu]_3$ (**5i**)[28b] was afforded in low yield (typically 19%), and significant amounts of $BH(NH^tBu)_2$ (**7i**) and $B_2H_5(\mu$-$NH^tBu)$ (**8i**, 55%)[30] were produced in the chromium-catalyzed dehydrogenation of **1i**. The tungsten-catalyzed reaction of **1i** was very slow. When an equimolar amount of the carbonyl complex was used, intense signals assignable to a borane complex, $[W(CO)_5(\eta^1$-$BH_3\cdot NH_2{}^tBu)]$, appeared during the photoreaction, indicating rather high stability of this species.

Stoichiometric Reaction between 1a and $[Cr(CO)_6]$. To know what occurs during the dehydrogenation process, a stoichiometric reaction of **1a** with $[Cr(CO)_6]$ was carried out and was carefully monitored by NMR spectroscopy. The ^{11}B NMR spectral change is displayed in Figure 1. After 1 min of photolysis, a significant amount of **1a** was consumed, and compound **2a** (δ ^{11}B = 5.0 ppm) formed. Monomeric BH_2=NMe_2 (**4a**, 37.5 ppm)[21c] and a small amount of trimeric $[BH_2NMe_2]_3$ (**6a**, 1.8 ppm)[23] were also observed. At this time, the ^1H NMR spectrum (Figure 1, inset) exhibited a new broad hump at −3.3 ppm. This is assigned to the BH protons of the borane σ complex, $[Cr(CO)_5(\eta^1$-$BH_3\cdot NHMe_2)]$ (**3a**), in which dimethylamineborane is coordinated to the chromium atom through a B−H−Cr single bridge. The hump is characteristic for the BH hydrogen atoms of borane complexes $[M(CO)_5(\eta^1$-$BH_3\cdot L)]$, in which the coordinated and terminal BH hydrogen atoms rapidly exchange.[13,31] The chemical shift value, −3.3 ppm, corresponds to the weighted average of those of the BH protons. In ^{11}B NMR, **3a** resonates at higher field by 3.6 ppm (−16.8 ppm) relative to free **1a**. Such high field shifts of the ^{11}B NMR signal have also been encountered in the formation of other borane complexes, $[M(CO)_5(\eta^1$-$BH_3\cdot L)]$,[13] $[CpMn(CO)_2(\eta^1$-$BH_3\cdot L)]$,[32] $[Mn(CO)_4(PR_3)(\eta^1$-$BH_3\cdot PMe_3)]^+$,[33] and $[CpRu(PMe_3)_2(\eta^1$-$BH_3\cdot L)]^+$ (L = tertiary phosphine and amine).[34] Compound **3a** decomposed so rapidly, liberating the aminoborane and H_2, that it could not be isolated. However, its structure was computationally deduced by geometry optimization based on density functional theory (DFT, see later).

After 5 min of photolysis, the signal of **4a** decreased in intensity while that of **2a** grew. In the ^1H NMR spectrum, a new boron-coupled broad quartet appeared at −4.79 ppm. This is assignable to the BH signal of $[Cr(CO)_5(\eta^1$-$BH_2NMe_2BH_2NMe_2)]$ (**9a**), which should be formed through complexation between $[Cr(CO)_5]$ and **2a** generated in the reaction system. Formation of **9a** was confirmed by a separate experiment: when $[Cr(CO)_6]$ was photolyzed in the presence of **2a** in C_6D_6, **9a** was observed by NMR as expected. The ^{11}B NMR spectrum of this solution exhibits two triplet resonances at 4.7 ppm, close to free **2a** (5.0 ppm), and at −2.4 ppm, higher field relative to **2a**. When a toluene-d_8 solution of **9a** was cooled to −80 °C, the high-field ^1H NMR resonance collapsed into the baseline. Further cooling to −90 °C revealed a new broad resonance, assigned to the chromium-coordinated hydrogen atom, at −12.0 ppm with 1H intensity. This indicates mono-

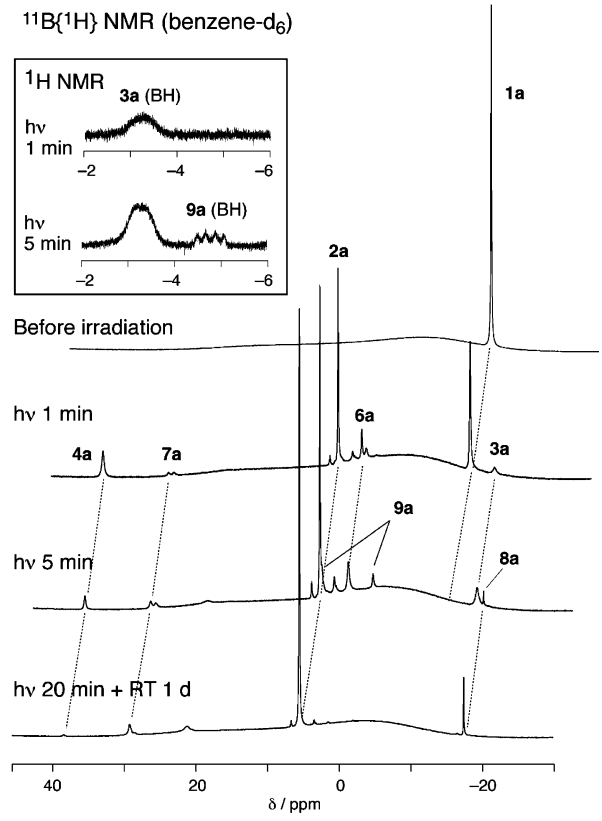

Figure 1. ^{11}B NMR (inset: ^1H NMR) spectral change during the dehydrocoupling reaction of **1a** catalyzed by $[Cr(CO)_6]$. **1a**: $BH_3\cdot NHMe_2$, **2a**: $[BH_2NMe_2]_2$, **3a**: $[Cr(CO)_5(\eta^1$-$BH_3\cdot NHMe_2)]$, **4a**: BH_2=NMe_2, **6a**: $[BH_2NMe_2]_3$, **7a**: $BH(NMe_2)_2$, **8a**: $B_2H_5(\mu$-$NMe_2)$, **9a**: $[Cr(CO)_5(\eta^1$-$BH_2NMe_2BH_2NMe_2)]$.

(29) Dietrich, B. L.; Goldberg, K. I.; Heinekey, D. M.; Autrey, T.; Linehan, J. C. *Inorg. Chem.* **2008**, *47*, 8583.
(30) Schwartz, L. D.; Keller, P. C. *J. Am. Chem. Soc.* **1972**, *94*, 3015.
(31) Kawano, Y.; Kakizawa, T.; Yamaguchi, K.; Shimoi, M. *Chem. Lett.* **2006**, *35*, 568.
(32) Kakizawa, T.; Kawano, Y.; Shimoi, M. *Organometallics* **2001**, *20*, 3211.
(33) Yasue, T.; Kawano, Y.; Shimoi, M. *Angew. Chem., Int. Ed.* **2003**, *42*, 1727.
(34) Kawano, Y.; Hashiva, M.; Shimoi, M. *Organometallics* **2006**, *25*, 4420.

Scheme 1

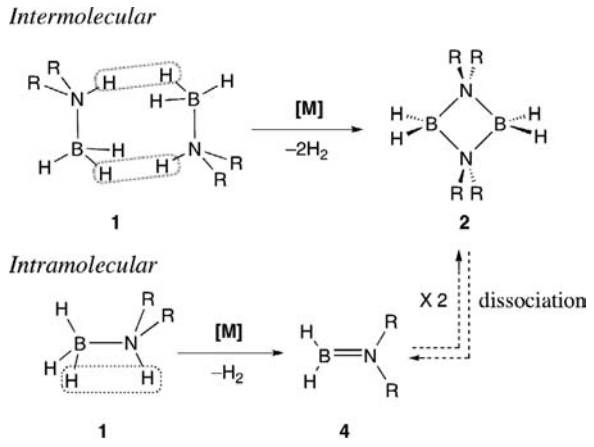

dentate coordination of the $[BH_2NMe_2]_2$ ligand and rapid exchange between the *geminal* BH hydrogen atoms (eq 5). The terminal BH signal coincided with that of free **2a** and could not be clearly observed. For this fluxional process, the free energy of activation was evaluated to be 7.4 kcal mol^{-1} at 193 K. The interboron exchange was not observed up to 25 °C. Such behavior of **9a** is closely related to that of diborane(4) derivatives, $[M(CO)_5(\eta^1\text{-}B_2H_4\cdot 2PMe_3)]$ (M = Cr, W). In these compounds, the site exchange between the *vicinal* BH hydrogen atoms is much slower than that between the *geminal* BH protons.[17,35] Unfortunately, isolation of **9a** was frustrated because of its lability.[36]

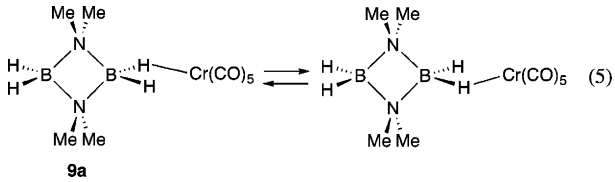

After the irradiation was terminated, the resonances of **9a** disappeared, while that of free **2a** further increased due to dissociation of the $[BH_2NMe_2]_2$ ligand from the metal. In the latter stage of the reaction, resonances of minor products, $BH(NMe_2)_2$ (**7a**, 28.5 ppm) and $B_2H_5(\mu\text{-}NMe_2)$ (**8a**, −18.0 ppm) appeared. These species are known to be generated by disproportionation of **4a**.[37,38]

Reaction Mechanism of the Dehydrocoupling: Intramolecular or Intermolecular. To discuss the reaction mechanism of the dehydrocoupling, it is necessary to consider two possible pathways, intermolecular and intramolecular reactions (Scheme 1). In the former mechanism, one of the hydridic BH atoms of **1** interacts in the coordination sphere with the acidic NH proton of another molecule to release H_2, forming a B−N covalent bond. On the other hand, in the latter process, BH and NH hydrogen atoms are eliminated from the same molecule to afford monomeric **4** and H_2. The monomer then dimerizes to provide **2** if the substituents are small.

Noncatalytic dehydrogenation of adduct **1a** at elevated temperature[39] was originally reported to occur through an intramolecular mechanism.[40] However, a bimolecular process was later suggested for this reaction on the basis of results obtained from deuterium-labeling experiments conducted by Ryschkewitsch and Wiggins.[41] A vacuum pyrolysis study by Manners also supported the intermolecular pathway.[26] Separately, for hydrogen elimination from ammoniaborane, quantum chemical calculations have shown an intramolecular pathway, which can be catalyzed by BH_3 generated by B−N dissociation.[42,43]

Intramolecular H_2 abstraction was suggested by Autrey and co-workers for $[RhCl(cod)]_2$-catalyzed dehydrocoupling of **1a** (cod = 1,5-cyclooctadiene).[44] They inferred that the active species were soluble Rh_{4-6} clusters based on solution XAFS and ^{11}B NMR study. In contrast, for the same reaction, Manners and co-workers proposed a mechanism involving intermolecular B−N coupling,[26] which occurs on the surface of in situ generated colloidal metal.[45,46] Autrey later suggested that with the progress of the dehydrocoupling, the rhodium clusters assembled with aminoborane-derived bridging ligands to generate insoluble polynuclear Rh complexes, which were oxidized to give metallic rhodium.[47] For the titanocene-catalyzed dehydrocoupling of **1a**, originally reported by Manners,[48] an intramolecular reaction mechanism was proposed by Ohno based on DFT calculations (*vide infra*).[49] Likewise, Chirik and coworkers suggested an intramolecular pathway for their titanocene- and zirconocene-catalyzed reactions.[50]

In the current group-6 metal-catalyzed system, the aminoborane products appear to be generated through the intramolecular process because of the formation of monomeric products in the dehydrogenation of bulky boranes, **1d** and **1e**. This is rationalized by the tungsten-catalyzed reaction of **1f**, which showed formation of $BH_2{=}NEt_2$ (**4f**) and its slow dimerization giving **2f**. Detection of **4a** at an earlier stage of the stoichiometric reaction of **1a** with $[Cr(CO)_6]$ also supports the initial formation of the monomer and its subsequent dimerization.

Computational Study. To obtain further insights into the reaction mechanism, we conducted theoretical calculations.

(35) Shimoi, M.; Katoh, K.; Kodama, G.; Kawano, Y.; Ogino, H. *J. Organomet. Chem.* **2002**, *659*, 102.
(36) Quite recently, a rhodium complex of $[BH_2NMe_2]_2$ was isolated and structurally characterized. The cyclic aminoborane is ligated to the rhodium atom in a bidentate fashion in this compound. Douglas, T. M.; Chaplin, A. B.; Weller, A. S. *J. Am. Chem. Soc.* **2008**, *130*, 14432. This report also described the formation of a rhodium−dimethylamineborane complex and its intermediacy in the Rh-catalyzed borane dehydrocoupling reaction.
(37) Nöth, H.; Vahrenkamp, H. *Chem. Ber.* **1966**, *99*, 1049.
(38) Hall, R. E.; Schram, E. P. *Inorg. Chem.* **1971**, *10*, 192.
(39) Niedenzu, K.; Dawson, J. W. *Boron-Nitrogen Compounds*; Academic Press Inc.: New York, 1965.
(40) Beachley, O. T., Jr. *Inorg. Chem.* **1967**, *6*, 870.
(41) Ryschkewitsch, G. E.; Wiggins, J. W. *Inorg. Chem.* **1970**, *9*, 314.
(42) (a) Nguyen, M. T.; Nguyen, V. S.; Matus, M. H.; Gopakumar, G.; Dixon, D. A. *J. Phys. Chem. A* **2007**, *111*, 679. (b) Li, Q. S.; Zhang, J.; Zhang, S. *Chem. Phys. Lett.* **2005**, *404*, 100.
(43) It has been proposed that the solid state thermolysis of ammoniaborane proceeds via an intermolecular pathway. This reaction provides H_2 and polymeric aminoborane $[BH_2NH_2]_x$. (a) Smith, R. S.; Kay, B. D.; Schmid, B.; Li, L.; Hess, N.; Gutowski, M.; Autrey, T. *Prep. Pap.−Am. Chem. Soc., Div. Fuel Chem.* **2005**, *50*, 112. (b) Stowe, A. C.; Shaw, W. J.; Linehan, J. C.; Schmid, B.; Autrey, T. *Phys. Chem. Chem. Phys.* **2007**, *9*, 1831.
(44) Chen, Y.; Fulton, J. L.; Linehan, J. C.; Autrey, T. *J. Am. Chem. Soc.* **2005**, *127*, 3254.
(45) In a recent review, they mentioned the possibility of an intramolecular mechanism. Clark, T. J.; Lee, K.; Manners, I. *Chem. Eur. J.* **2006**, *12*, 8634.
(46) (a) Jaska, C. A.; Manners, I. *J. Am. Chem. Soc.* **2004**, *126*, 1334. (b) Jaska, C. A.; Manners, I. *J. Am. Chem. Soc.* **2004**, *126*, 9776. (c) Jaska, C. A.; Clark, T. J.; Clendenning, S. B.; Grozea, D.; Turak, A.; Lu, Z.-H.; Manners, I. *J. Am. Chem. Soc.* **2005**, *127*, 5116.
(47) Fulton, J. F.; Linehan, J. C.; Autrey, T.; Balasubramanian, M.; Chen, Y.; Szymczak, N. K. *J. Am. Chem. Soc.* **2007**, *129*, 11936.
(48) Clark, T. J.; Russell, C. A.; Manners, I. *J. Am. Chem. Soc.* **2006**, *128*, 9582.
(49) Luo, Y.; Ohno, K. *Organometallics* **2007**, *26*, 3597.
(50) Pun, D.; Lobkovsky, E.; Chirik, P. J. *Chem. Commun.* **2007**, 3297.

Scheme 2. Free-Energy Profile for Borane Dehydrocoupling via **3a** (Path I)[a]

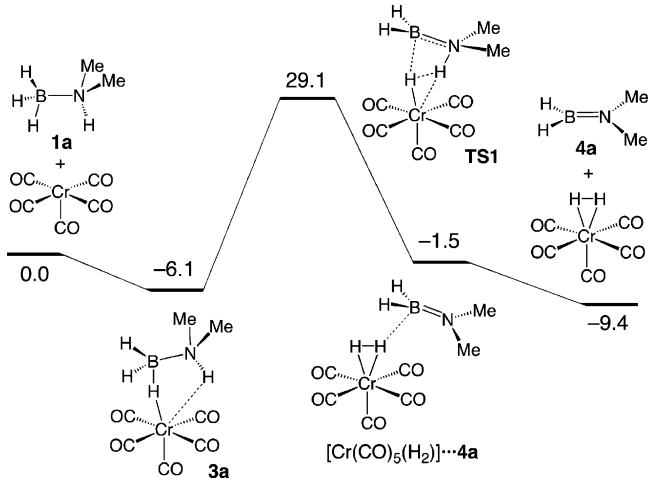

[a] The solvation free energies (kcal mol^{-1}, 298 K, 1 atm) were evaluated at the PBE0/SDD (Cr), aug-cc-pVDZ (other atoms) level using the CPCM model (solvent = benzene).

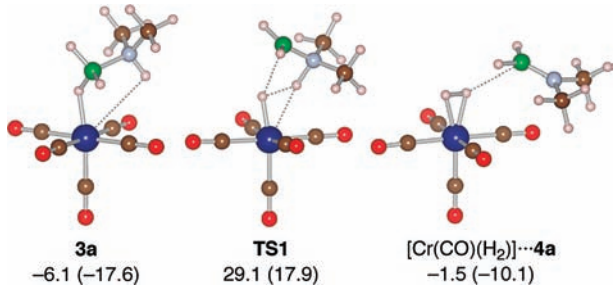

Figure 2. DFT-optimized structures of **3a**, **TS1**, and [Cr(CO)$_5$(H$_2$)]···**4a**. Free energies relative to the separated reactants, **1a** + [Cr(CO)$_5$], are given in kcal mol^{-1}. Zero-point-corrected electronic energies are also given in parentheses. Throughout this paper, indigo = Cr, brown = C, red = O, green = B, blue gray = N, pink = H.

Geometry optimizations and vibration analyses were performed by the DFT method with use of the PBE0 functional.[51] The single-point energies in solution were then calculated with larger basis sets (see Experimental Section) applying the CPCM model[52] to the optimized geometries. First, we describe the intramolecular process, which was suggested in the former section.

Intramolecular Reaction. As mentioned already, a borane σ complex **3a** is observed during the Cr-catalyzed dehydrocoupling reaction of **1a**. Scheme 2 shows the free energy profile (ΔG_{sol}) of an intramolecular reaction pathway containing this complex as an intermediate (path I). The structures of each species are exhibited in Figure 2. This mechanism involves concerted hydrogen elimination. In complex **3a**, the borane ligand coordinates to chromium through a B−H−Cr single bridge, and the NH proton also has a hydrogen-bond-like interaction with a filled chromium d orbital.[53] The B−H$_{coord}$, Cr−H, and NH···Cr interatomic distances are 1.268, 1.772, and 3.202 Å, respectively. In the transition state (**TS1**), the NH proton is drawn toward the metal center, and the coordinated BH bond is significantly stretched (B···H(Cr) 2.460 Å). The NH proton further approaches the chromium atom leaving an aminoborane molecule to produce a dihydrogen complex [Cr(CO)$_5$(H$_2$)].[54] Importantly, this process has a large free energy of activation, 35.2 kcal mol^{-1} and, thus, is not suitable for the borane dehydrocoupling, which progresses smoothly at ambient temperature. Despite repeated trials, we could not find a plausible reaction mechanism that goes through **3a**.

DFT calculations suggest that the active species of this reaction was [Cr(CO)$_4$]. Scheme 3 illustrates the reaction mechanism of the [Cr(CO)$_4$]-catalyzed dehydrocoupling (path II). The optimized structures and geometrical parameters of the concerned species are presented in Figure 3 and Table 3, respectively. This reaction proceeds via a stepwise mechanism involving both NH and BH bond activation. Borane **1a** coordinates to [Cr(CO)$_4$] through the BH and NH hydrogen atoms to generate a chelate complex **10a**. The formation of **10a** is 2.6 kcal mol^{-1} endergonic, and 9.9 kcal mol^{-1} favorable in electronic energy. Complex **10a** undergoes NH insertion to generate **11a** through **TS2** having an N−H−Cr three-center interaction. **11a** contains an amido-borane ligand which coordinates to the chromium atom through the nitrogen lone electron pair and a BH bond.[55] The energy barrier for the NH activation is 9.1 kcal mol^{-1}, so this process occurs very easily. Subsequently, BH activation takes place to produce **12a**. After this step Cr-mediated H$_2$ elimination of **1a** has been attained, and an aminoborane moiety is formed on the metal center. During the transformation from **11a** to **12a**, the BH$_2$NMe$_2$ group rotates 90° around the Cr−N axis, leaving a hydride which was hitherto bound to boron. In the key species **12a**, the two hydrides, which were originally from the BH and NH protons, are mutually equivalent. This BH activation is the rate-determining step in the whole catalytic reaction, and its energy barrier is 13.3 kcal mol^{-1}. This value is significantly reduced in comparison to those for the noncatalytic and BH$_3$-catalyzed intramolecular dehydrogenation of **1a**, 40.2 and 26.9 kcal mol^{-1}, respectively (Scheme 4).

As found in Table 3, in the chelate complex **10a** the Cr−H(N) bond distance (1.917 Å) is substantially longer than that of the Cr−H(B) bond (1.766 Å). This reflects the weak coordination of the protonic NH hydrogen atom. During the NH activation step, the NH bond is greatly elongated (**10a** 1.055, **TS2** 1.480, **11a** 2.458 Å), while the BH interatomic distance does not change very much. However, the latter is increased dramatically in the subsequent BH activation step. In **11a**, **TS3**, and **12a**, the BH separations are 1.378, 2.305, and 2.825 Å, respectively.

(51) Perdew, J. P.; Burke, K.; Ernzerhof, M. *Phys. Rev. Lett.* **1996**, *77*, 3865.
(52) (a) Barone, V.; Cossi, M. *J. Phys. Chem. A* **1998**, *102*, 1995. (b) Cossi, M.; Rega, N.; Scalmani, G.; Barone, V. *J. Comput. Chem.* **2003**, *24*, 669.
(53) Selected papers for M···HX hydrogen bonds: (a) Brammer, L.; McCann, M. C.; Bullock, R. M.; McMullan, R. K.; Sherwood, P. *Organometallics* **1992**, *11*, 2339. (b) Roe, D. M.; Bailey, P. M.; Moseley, K.; Maitlis, P. M. *J. Chem. Soc., Chem. Commun.* **1972**, 1273.
(54) (a) Matthews, S. L.; Pons, V.; Heinekey, D. M. *J. Am. Chem. Soc.* **2005**, *127*, 850. (b) Sweany, R. L. *J. Am. Chem. Soc.* **1985**, *107*, 2374. (c) Upmacis, R. K.; Gadd, G. E.; Poliakoff, M.; Simpson, M. B.; Turner, J. J.; Whyman, R.; Simpson, A. F. *J. Chem. Soc., Chem. Commun.* **1985**, 27. (d) Church, S. P.; Grevels, F.-W.; Hermann, H.; Schaffner, K. *J. Chem. Soc., Chem. Commun.* **1985**, 30.
(55) Quite recently, a related zirconocene−amidoborane complex was isolated and structurally characterized. Forster, T. D.; Tuononen, H. M.; Parvez, M.; Roesler, R. *J. Am. Chem. Soc.* **2009**, *131*, 6689. Harder's amidoborane calcium compound is also relevant. Spielmann, J.; Harder, S. *J. Am. Chem. Soc.* **2009**, *131*, 5064. In addition, a lutetium imine-stabilized borane complex, which was reported by Roesky and coworkers very recently, has structural relevance. Meyer, N.; Jenter, J.; Roesky, P. W.; Eickerling, G.; Scherer, W. *Chem. Commun.* **2009**, 4693.

Scheme 3. Free-Energy Profile for the Borane Dehydrocoupling Catalyzed by $[Cr(CO)_4]$ (path II)[a]

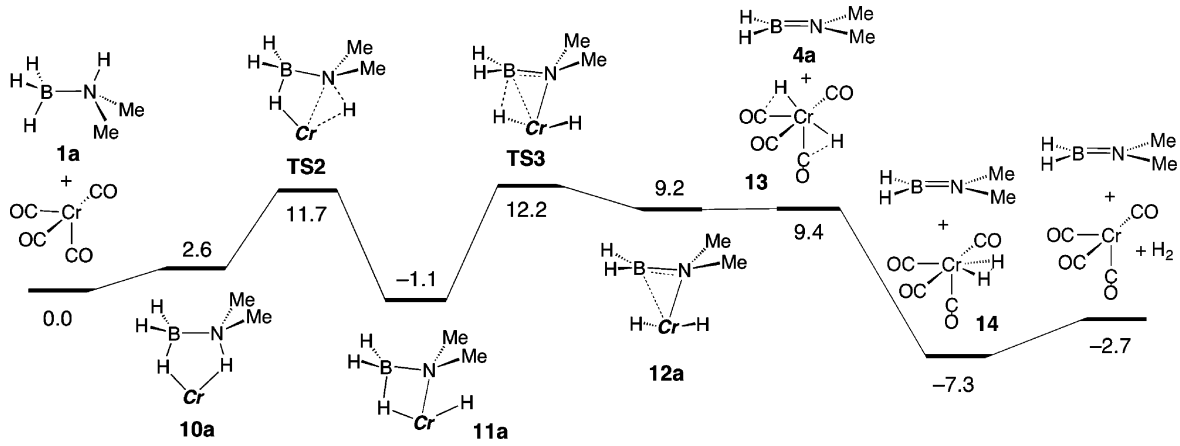

[a] ***Cr*** denotes $[Cr(CO)_4]$.

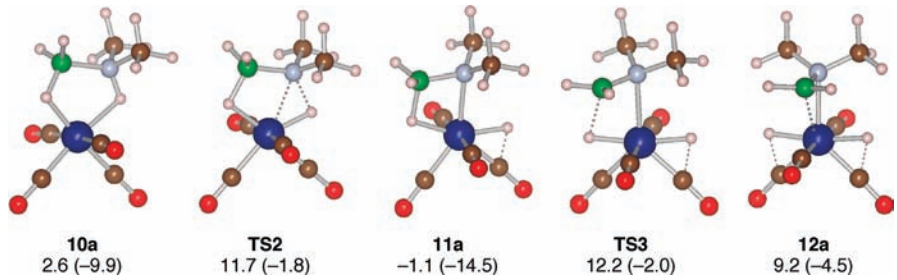

Figure 3. DFT-optimized structures of **10a**, **TS2**, **11a**, **TS3**, and **12a**. Free energies relative to the separated reactants, **1a** + $[Cr(CO)_4]$, are given in kcal mol^{-1} (zero-point-corrected electronic energies are given in parentheses).

Table 3. Calculated Interatomic Distances (Å) for **10a**, **TS2**, **11a**, **TS3**, and **12a**

	10a	TS2	11a	TS3	12a
B−H_{cood}	1.275	1.334	1.378	2.305	2.825
N−H	1.055	1.480	2.458	2.659	2.625
Cr−B	2.428	2.337	2.380	2.516	2.416
Cr−N	2.442	2.142	2.099	2.229	2.175
Cr−H(B)	1.766	1.728	1.703	1.634	1.650
Cr−H(N)	1.917	1.573	1.619	1.649	1.650
B−N	1.653	1.570	1.518	1.448	1.457

Scheme 4. Non-Catalytic and BH_3-Catalyzed Intramolecular Dehydrogenation Reactions of **1a**. Relative Solvation Free Energies (zero-point-corrected electronic energies) are given in kcal mol^{-1}

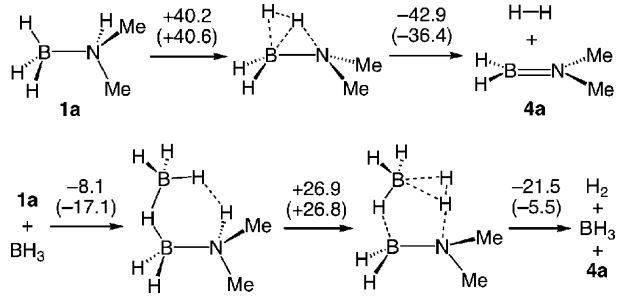

In **12a**, the B−N bond length, 1.457 Å, is an intermediate value between the corresponding bond lengths of **1a** (1.610 Å) and **4a** (1.388 Å). In addition, the boron and nitrogen atoms are slightly pyramidalized. The aminoborane ligand coordinates to the chromium atom through the nitrogen electron pair with a Cr−N bond distance of 2.175 Å. At the same time, the Cr···B distance is 2.416 Å, suggesting the contribution of metal back-donation into the boron p orbital.

Scheme 5. Free-Energy Profile for the Isomerization of **13** to **14**

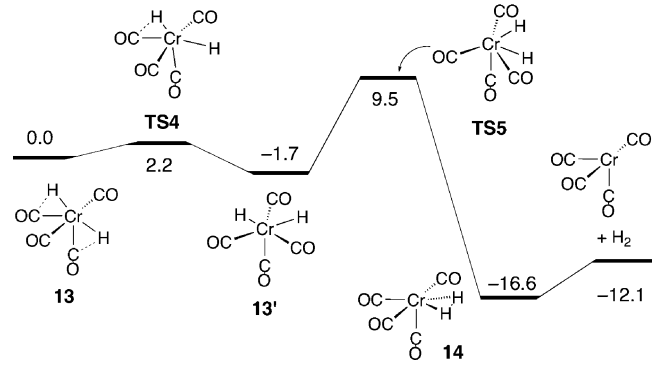

Aminoborane dissociation from **12a** is a barrierless process, and almost neutral in free energy. The resulting dihydride **13** cannot release H_2 itself because of the *trans* configuration of the two hydride ligands. However, it can isomerize with deformation of the ligand arrangement. The resultant dihydrogen adduct **14** releases H_2 rapidly to regenerate the active species $[Cr(CO)_4]$. Scheme 5 and Figure 4 depict the isomerization of **13** to **14**. It proceeds in two steps, where the highest reaction barrier is 11.1 kcal mol^{-1} for the second step from **13′** to **14**.

Coordinatively unsaturated $[Cr(CO)_4]$ is known to be generated photochemically.[56] We found that it was also generated thermally in the reaction system (Scheme 6 and Figure 5). Two molecules of $[Cr(CO)_5]$, formed from dissociation of borane

(56) Fletcher, T. R.; Rosenfeld, R. N. *J. Am. Chem. Soc.* **1985**, *107*, 2203.

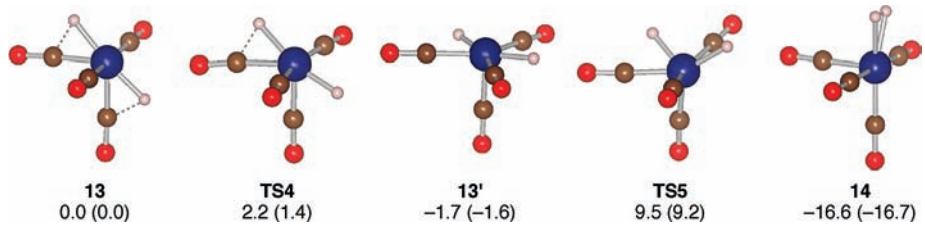

Figure 4. DFT-optimized structures of the isomers of $[Cr(CO)_4H_2]$ and transition states connecting them. Relative free energies are given in kcal mol^{-1}. Zero-point-corrected electronic energies are given in parentheses.

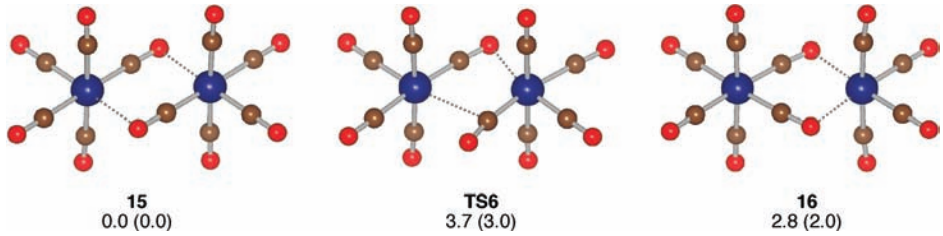

Figure 5. DFT-optimized structures of **15**, **TS6**, and **16**. Relative free energies are given in kcal mol^{-1}. Zero-point-corrected electronic energies are given in parentheses.

Scheme 6. Free-Energy Profile for the Isomerization of the Dihydride **13** to the Dihydrogen Complex **14**

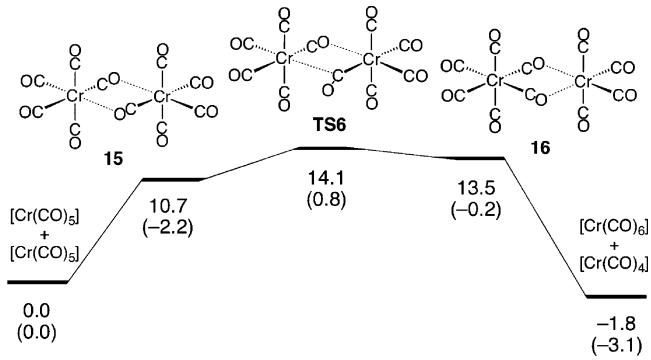

from **3a** or photolysis of $[Cr(CO)_6]$, associate to give a loosely bound dimer **15**. In **15**, $[Cr(CO)_5]$ fragments donate electron density to each other from a carbonyl oxygen atom, where the Cr···Cr and Cr···O separations are 3.812 and 2.395 Å, respectively. One of the bridging carbonyl ligands then turns and migrates between the two chromium atoms to afford $[Cr(CO)_6]$···$[Cr(CO)_4]$ (**16**).[57] The transition state connecting **15** and **16**, **TS6**, is only 3.4 kcal mol^{-1} higher than **15** and 14.1 kcal mol^{-1} higher than the separated reactants (two molecules of $[Cr(CO)_5]$) in free energy, so that this process can readily occur under ambient conditions to release the active catalyst into the solution. The thermal generation of $[Cr(CO)_4]$ readily explains that the dehydrocoupling of **1a** is catalyzed by $[Cr(CO)_5(thf)]$ or $[Cr(CO)_5(\eta^1\text{-}BH_3{\cdot}NMe_3)]$ and progresses smoothly in the dark.

The role of the σ complex **3a** in the catalytic cycle should also be considered. This complex acts as a reservoir of $[Cr(CO)_5]$ in the reaction mixture. Complex **3a** readily releases the borane ligand with a reaction free energy of 6.1 kcal mol^{-1}.[58] Hence, $[Cr(CO)_5]$, the source of the active catalyst, is supplied even after the irradiation is switched off.

Recently, Luo and Ohno reported a theoretical treatment of the titanocene-catalyzed dehydrocoupling of **1a**.[49] In this reaction, the borane first coordinates to a $TiCp_2$ fragment to generate an adduct, $[Cp_2Ti(\eta^1\text{-}BH_3{\cdot}NHMe_2)]$. Similarly to the current Cr-catalyzed reaction, the dehydrogenation of this complex proceeds via a stepwise mechanism including NH cleavage followed by BH cleavage. In contrast, however, a concerted H_2 elimination mechanism has been shown for the H_2 elimination of ammoniaborane by an iridium pincer catalyst.[59]

Intermolecular Reaction. We also computed the intermolecular reaction pathway (path III). The acidity of the NH proton may be enhanced in complex **3a** because of the borane polarization induced by the metal coordination. The dehydrogenation could be initiated through the electrostatic interaction of the acidic NH proton with a hydridic BH of another molecule of **1a** in the reaction system. Indeed, a related intermolecular reaction mechanism has been proposed by Denis for dehydrocoupling of phosphineboranes catalyzed by $B(C_6F_5)_3$.[60]

To form such an intermolecular NH···HB dipole−dipole interaction, the metal-coordinated dimethylamineborane needs to point the NH proton toward the incoming molecule of **1a**. Such a geometry is realized in an isomer of the borane complex, **3a′** (Scheme 7). Association of **3a′** with free **1a** occurs through "dihydrogen bonds"[61,62] to produce adduct **3a′···1a**. The adduct formation is only 2.8 kcal mol^{-1} endergonic. In **3a′···1a**, the BH···HN interatomic distances are 1.937−2.065 Å. Similar association through BH···HN interactions has been demonstrated in the crystal structures of $BH_3{\cdot}NR_2BH_2{\cdot}NHR_2$ (R =

(57) The existence of $[Cr_2(CO)_{10}]$ after photolysis of $[Cr(CO)_6]$ has been suggested. Fletcher, T. R.; Rosenfeld, R. N. *J. Am. Chem. Soc.* **1985**, *107*, 2203.

(58) Labile nature of borane ligands has been confirmed experimentally. Kawano, Y.; Yamaguchi, K.; Miyake, S.; Kakizawa, T.; Shimoi, M. *Chem.—Eur. J.* **2007**, *13*, 6920.

(59) Paul, A.; Musgrave, C. B. *Angew. Chem., Int. Ed.* **2007**, *46*, 8153.

(60) Denis, J.-M.; Fointos, H.; Szelke, H.; Toupet, L.; Pham, T.-N.; Madec, P.-J.; Gaumont, A.-C. *Chem. Commun.* **2003**, 54.

(61) Bakhmutov, V. I. *Dihydrogen Bond, Principles, Experiments, and Applications*; Wiley-VCH: New York, 2008.

(62) Selected papers for dihydrogen bond: (a) Crabtree, R. H.; Siegbahn, P. E. M.; Eisenstein, O.; Rheingold, A. L.; Koetzle, T. F. *Acc. Chem. Res.* **1996**, *29*, 348. (b) Crabtree, R. H. *Science* **1998**, *282*, 2000. (c) Bosque, R.; Maseras, F.; Eisenstein, O.; Patel, B. P.; Yao, W.; Crabtree, R. H. *Inorg. Chem.* **1997**, *36*, 5505. (d) Lee, J. C., Jr.; Peris, E.; Rheingold, A. L.; Crabtree, R. H. *J. Am. Chem. Soc.* **1994**, *116*, 11014. (e) Xu, W.; Lough, A. J.; Morris, R. H. *Inorg. Chem.* **1996**, *35*, 1549.

Scheme 7. Intermolecular Dehydrogenation of **1a** on Chromium (Path III)[a]

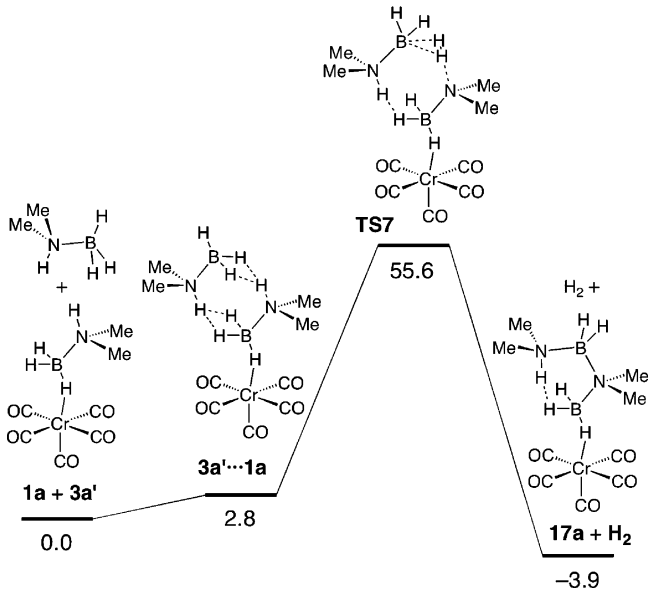

[a] Relative solvation free energies are given in kcal mol^{-1}.

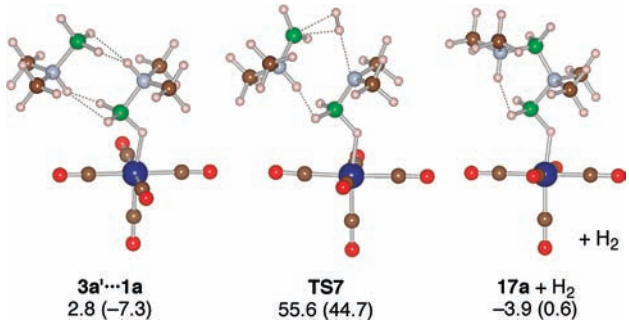

Figure 6. DFT-optimized structures of species regarding path III. Solvation free energies and zero-point-corrected electronic energies (in parentheses) relative to the separated reactants (**3a′** + **1a**) are given in kcal mol^{-1}.

Me, 1/2$(CH_2)_4$).[26,63,64] Some phosphineboranes and hybrid amineborane−phosphineborane species also show analogous structural motifs.[65,66]

It is likely that the intermolecular reaction proceeds through adduct **3a′···1a**. This complex successively releases two equivalents of H_2. In the first step, the acidic NH proton of the ligated amineborane approaches one of the BH hydrogen atoms of associated **1a** to form an H−H bond (**TS7**, see Scheme 7 and Figure 6). In **TS7**, the H_2 moiety interacts with a boron atom in an η^2-fashion. This is reminiscent of the structure of

Scheme 8. Non-catalytic, intermolecular dehydrocoupling of **1a**[a]

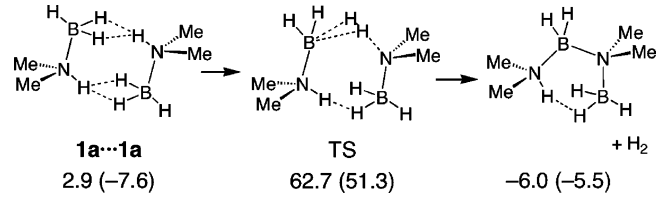

[a] Solvation free energies and zero-point-corrected electronic energies (in parentheses) relative to the separated reactants (two molecules of **1a**) are given in kcal mol^{-1}.

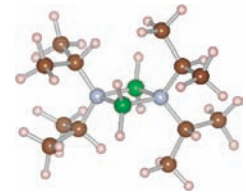

Figure 7. DFT (PBE0)-optimized structure of **2d**.

$BH_3(\eta^2$-$H_2)$, which has been observed in cryogenic matrices.[67,68] H_2 release via **TS7** results in the formation of a B−N covalent bond to afford the coupling product **17a**. This step is 3.9 kcal mol^{-1} exergonic, and the activation barrier is slightly reduced again compared with the noncatalytic reaction (Scheme 8). Nonetheless, its value 52.8 kcal mol^{-1} is still very large, and therefore, this type of intermolecular reaction is unlikely to contribute to the borane dehydrocoupling.[69]

As noted above, the $[Cr(CO)_4]$-catalyzed intramolecular reaction mechanism, path II, is strongly suggested for the catalytic dehydrocoupling of **1a**. Neither path I, which goes via **3a**, nor path III, the intermolecular reaction pathway, are favorable. Other computed possibilities for the reaction mechanism are presented in Supporting Information.

Dehydrogenation Reactions of Bulky Boranes. Finally, we discuss the reactions of boranes containing bulky substituents. In the NH activation step of path II, the amine moiety necessarily approaches the metal center. As this occurs, bulky substituents on nitrogen can give rise to steric repulsion between the amine group and metal fragment to destabilize the transition state. This explains the slow reaction of the bulky boranes.

Dimerization of methyl-substituted aminoborane **4a** is 3.6 kcal mol^{-1} favorable in free energy. In contrast, that of the isopropyl derivative **4d** is endergonic by 17.2 kcal mol^{-1}. Indeed, its dimer **2d** has a highly congested structure involving cross-ring steric interaction between the isopropyl groups, as shown by the DFT-based geometry optimization (Figure 7).

Conclusion

In this paper, we described the dehydrocoupling reactions of borane−secondary amine adducts, **1a**−**f**, catalyzed by $[M(CO)_6]$

(63) Nöth, H.; Thomas, S. *Eur. J. Inorg. Chem.* **1999**, 1373.
(64) In crystal, free **1a** adopts a chain-like structure, in which amineborane molecules are linked by BH···HN interactions. Molecules of primary adduct **1g** are linked in ribbons. Aldridge, S.; Downs, A. J.; Tang, C. Y.; Parsons, S.; Clarke, M. C.; Johnstone, R. D. L.; Robertson, H. E.; Rankin, D. W. H.; Wann, D. A. *J. Am. Chem. Soc.* **2009**, *131*, 2231.
(65) Dorn, H.; Singh, R. A.; Massey, J. A.; Nelson, J. M.; Jaska, C. A.; Lough, A. J.; Manners, I. *J. Am. Chem. Soc.* **2000**, *122*, 6669. This paper also reported Rh-catalyzed dehydrocoupling reactions of phosphine boranes.
(66) Jaska, C. A.; Lough, A. J.; Manners, I. *Inorg. Chem.* **2004**, *43*, 1090.
(67) (a) Tague, T. J., Jr.; Andrews, L. *J. Am. Chem. Soc.* **1994**, *116*, 4970. (b) Watts, J. D.; Bartlett, R. J. *J. Am. Chem. Soc.* **1995**, *117*, 825. (c) Schreiner, P. R.; Schaefer, H. F.; Schleyer, P. v. R. *J. Chem. Phys.* **1994**, *101*, 7625.
(68) It has been reported that the alcoholysis of BH_4^- takes place through a transition state involving a closely related $H_3B(\eta^2$-$H_2)\cdots OR^-$ structure. Filippov, O. A.; Filin, A. M.; Tsupreva, V. N.; Belkova, N. V.; Lledós, A.; Ujaque, G.; Epstein, L. M.; Shubina, E. S. *Inorg. Chem.* **2006**, *45*, 3086.
(69) In an additional note, the second H_2 elimination from **17a** does not lead to ring closure giving **9a**, but causes the formation of two equivalents of **4a** through the central B−N bond cleavage of the $BH_3{\cdot}NMe_2BH_2{\cdot}NHMe_2$ ligand (see Supporting Information). Hence, detection of monomeric aminoboranes **4** during the dehydrocoupling is not incompatible with the possibility of intermolecular reaction, although it has been excluded on the basis of the high activation barrier. The formation of two molecules of **4a** has also been pointed out by Ohno in the thermolysis of $BH_3{\cdot}NMe_2BH_2{\cdot}NHMe_2$. Luo, Y.; Ohno, K. *Organometallics* **2007**, *26*, 3597.

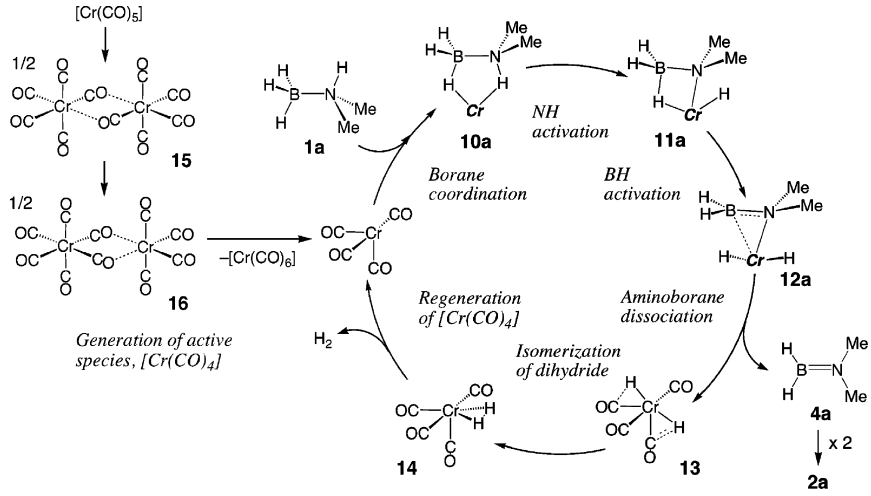

Figure 8. Catalytic cycle of the dehydrocoupling reaction of **1a**. ***Cr*** represents $[Cr(CO)_4]$.

under photolytic conditions. This reaction primarily produces aminoboranes **4a**−**f**. When the amine substituents are small, they dimerize to give cyclic boranes, $[BH_2NR_2]_2$ (**2a**−**c**, R = Me, $1/2C_4H_8$, $1/2C_5H_{10}$). In contrast, the dehydrogenation of bulky amineboranes afforded monomers, $BH_2{=}NR_2$ (**4d**, **e**; R = ^{i}Pr, Cy), as the main product.

The mechanism of this interesting reaction was investigated by DFT calculation. The borane dehydrocoupling reaction is catalyzed by $[Cr(CO)_4]$ and follows a stepwise intramolecular pathway (path II). The whole catalytic cycle is illustrated in Figure 8. It includes (i) generation of the active catalyst $[Cr(CO)_4]$, (ii) borane coordination and dehydrogenation on the chromium atom, and (iii) isomerization of the resulting dihydride complex (regeneration of the active species). All three of these processes take place with a reasonably low barrier. The borane σ complex **3a**, observed in the reaction mixture, acts as a reservoir of $[Cr(CO)_5]$, which is a source of the active species.

We also reported here the dehydrocoupling of primary adducts, $BH_3{\cdot}NH_2R$ (**1g**−**i**). These compounds underwent multiple dehydrogenations to produce borazine derivatives **5**. In the course of the borazine formation, aminoborane oligomers, $[BH_2NHR]_n$, are observed in the reaction mixture. Monomethylaminoborane is known to be the most stable in trimer, $[BH_2NHMe]_3$.[21a] It is plausible that the cyclic trimer is in equilibrium with the oligomers and that it undergoes metal coordination followed by hydrogen elimination to yield borazines.

Group-6 metal carbonyl complexes are commercially available and easy to handle. Furthermore, in this system, the reaction is not initiated only by mixing the chemicals, but is also triggered photochemically. Thus, the use of transition metal carbonyls may offer a more controllable catalytic system in borane dehydrocoupling reactions. Attempts to construct other such systems are currently underway.

Experimental Section

All manipulations were carried out under high vacuum or dry nitrogen atmosphere. Reagent-grade hexane, toluene, and THF were distilled under nitrogen atmosphere from sodium-benzophenone ketyl immediately before use. Benzene-d_6 and toluene-d_8 were dried over potassium mirrors and vacuum transferred into NMR tubes directly before use. $BH_3{\cdot}NHMe_2$ (**1a**), $BH_3{\cdot}NH(CH_2)_4$ (**1b**), $BH_3{\cdot}NH(CH_2)_5$ (**1c**), $BH_3{\cdot}NH^iPr_2$ (**1d**), $BH_3{\cdot}NHCy_2$ (**1e**), $BH_3{\cdot}NHEt_2$ (**1f**), $BH_3{\cdot}NH_2Me$ (**1g**), $BH_3{\cdot}NH_2Et$ (**1h**), and $BH_3{\cdot}NH_2{}^t$Bu (**1i**) were prepared by treatment of $NaBH_4$ with the corresponding ammonium salt in THF according to the literature.[70] $[Cr(CO)_6]$, $[Mo(CO)_6]$ (Strem), and $[W(CO)_6]$, $NaBH_4$ (Aldrich) were purchased and used as received. ^{1}H and ^{11}B NMR spectra were recorded on a JEOL FX-90Q or an α-500 spectrometer. IR spectra were recorded on a JASCO FTIR-350 or a Bruker IFS66v spectrometer.

Catalytic Preparation of $[BH_2NMe_2]_2$ (2a). Samples of $BH_3{\cdot}NHMe_2$ (**1a**) (1090 mg, 18.50 mmol) and $[Cr(CO)_6]$ (24 mg, 0.11 mmol) were dissolved in THF (7 mL). This solution was loaded in a Pyrex glass tube (20 mm o.d.) equipped with a high vacuum stopcock and irradiated using a 450 W medium pressure Hg lamp at 6 °C under vacuum. This led to vigorous gas evolution and yielded a yellow solution. After the irradiation for 1 h, the solution was stirred at room temperature for 24 h, and the resulting pale green suspension was then evaporated to dryness. From the solid residue, **2a** (726 mg, 6.38 mmol, 69%) was isolated by sublimation as a colorless crystalline solid (40 °C/1 × 10^{-4} torr). The ^{1}H and ^{11}B NMR spectral data accorded with literature values.[21]

Dehydrogenation of Borane−Secondary Amine Adducts. Typically, $BH_3{\cdot}NH(CH_2)_4$ (**1b**) (16 mg, 0.19 mmol) and $[Cr(CO)_6]$ (2.0 mg, 9.2 × 10^{-3} mmol) were dissolved in C_6D_6 (ca. 0.5 mL) and irradiated at 8 °C in a vacuum-sealed Pyrex NMR tube (5 mm o.d.). The progress of the dehydrogenation was monitored by ^{1}H and ^{11}B NMR spectroscopy. Dehydrocoupling of other borane adducts was carried out in similar fashion. The products were characterized by comparing the ^{1}H and ^{11}B NMR data with the literature.[21c,22−25]

During the reaction, borane σ complexes $[M(CO)_5(\eta^1\text{-}BH_3{\cdot}NHR_2)]$ were detected unless the molybdenum catalyst was employed. The tungsten-catalyzed dehydrogenation reaction of $BH_3{\cdot}NHCy_2$ (**1e**) was so slow that the formation of **4e** was not confirmed, but the borane complex $[W(CO)_5(\eta^1\text{-}BH_3{\cdot}NHCy_2)]$ was observed. In the reaction of **1a**−**c**, the complex of dimeric aminoborane, $[M(CO)_5(\eta^1\text{-}BH_2NR_2BH_2NR_2)]$, was also detected. The ^{1}H and ^{11}B NMR data for these complexes are presented in Table 4.

Dehydrogenation of Borane−Primary Amine Adducts. $BH_3{\cdot}NH_2Me$ (**1g**) (8.5 mg, 0.19 mmol) and $[Cr(CO)_6]$ (2.0 mg, 9.2 × 10^{-3} mmol) were dissolved in benzene-d_6 (ca. 0.5 mL) and irradiated at 8 °C using a 450 W medium pressure Hg lamp. The reaction was followed by ^{1}H and ^{11}B NMR spectroscopy. After 1 h of photolysis, a white viscous material precipitated and the reaction mixture exhibited a broad resonance at 0 to −10 ppm in the ^{11}B NMR spectrum. However, this precipitate disappeared by further irradiation and subsequent dark reaction. After 8 h of

(70) (a) Bonham, J.; Drago, R. S. *Inorg. Synth.* **1967**, *9*, 8. (b) Nöth, H.; Beyer, H. *Chem. Ber.* **1960**, *93*, 928. (c) Kelly, H. C.; Marchelli, F. R.; Giusto, M. B. *Inorg. Chem.* **1964**, *3*, 431.

Table 4. ^{1}H and ^{11}B NMR Spectral Data for Borane Complexes Observed in the Dehydrocoupling Reactions

cmpd	^{1}H NMR[a]	^{11}B NMR[a]
$[Cr(CO)_5(\eta^1\text{-}BH_3\cdot NHMe_2)]$ (**3a**)	3.30 (br, 1H, NH), 1.39 (d, $^{3}J_{HH}$ = 6.0 Hz, 6H, CH_3), −3.3 (br, 3H, BH_3)	−16.8 (br)
$[W(CO)_5(\eta^1\text{-}BH_3\cdot NHMe_2)]$	1.67 (d, $^{3}J_{HH}$ = 5.5 Hz, 6H, CH_3), −1.46 (br q, $^{1}J_{BH}$ = 102 Hz, 3H, BH_3)[b]	−20.6 (br)
$[Cr(CO)_5(\eta^1\text{-}BH_3\cdot NH(CH_2)_4)]$ (**3b**)	−3.06 (br q, $^{1}J_{BH}$ = 102 Hz, 3H, BH_3)[c]	−20.3 (br)
$[Cr(CO)_5(\eta^1\text{-}BH_3\cdot NH(CH_2)_5)]$ (**3c**)	3.0 (br, 1H, NH), 2.21, 1.63 (m, 2H × 2, NCH_2), 0.68, 0.1−0.3 (m, 3H × 2, CH_2), −3.36 (q, $^{1}J_{BH}$ = 90 Hz, 3H, BH_3)	−19.3 (br)
$[W(CO)_5(\eta^1\text{-}BH_3\cdot NH(CH_2)_5)]$	2.28, 1.66 (m, 2H × 2, NCH_2), 0.72, 0.30 (m, 3H × 2, CH_2), −1.54 (q, $^{1}J_{BH}$ = 70 Hz, 3H, BH_3)	−23.8 (br)
$[Cr(CO)_5(\eta^1\text{-}BH_3\cdot NH^iPr_2)]$	3.55 (m, 2H, CHMe$_2$), 0.83 (d, $^{3}J_{HH}$ = 6.4 Hz, 6H), 0.77 (d, $^{3}J_{HH}$ = 5.8 Hz, 6H) (diastereotopic CHMe_2), −3.04 (br, $^{1}J_{BH}$ = 110 Hz, 3H, BH)[d]	−25.2 (br)
$[W(CO)_5(\eta^1\text{-}BH_3\cdot NH^iPr_2)]$	3.15 (br, 1H, NH), 0.74 (d, $^{3}J_{HH}$ = 5.0 Hz, 6H), 0.64 (d, $^{3}J_{HH}$ = 7.0 Hz, 6H) (diastereotopic CHMe_2), −1.35 (q, br, 3H, BH)[c]	−29.1 (br)
$[Cr(CO)_5(\eta^1\text{-}BH_3\cdot NHCy_2)]$	−3.0 (br, 3H, BH_3)[b,e]	−23.9 (br)
$[W(CO)_5(\eta^1\text{-}BH_3\cdot NHCy_2)]$	−1.2 (br, 3H, BH_3)[b,e]	−28.4 (br)
$[Cr(CO)_5(\eta^1\text{-}BH_3\cdot NHEt_2)]$	1.90, 1.75 (m, 2H × 2, CH_2), 0.38 (t, $^{3}J_{HH}$ = 7.0 Hz, 6H, CH_3), −3.29 (q, 3H, $^{1}J_{BH}$ = 100 Hz, BH_3)	−20.9 (br)
$[W(CO)_5(\eta^1\text{-}BH_3\cdot NHEt_2)]$	1.89, 1.73 (m, 2H × 2, CH_2), 0.36 (t, $^{3}J_{HH}$ = 7.0 Hz, 6H, CH_3), −1.58 (q, 3H, $^{1}J_{BH}$ = 80 Hz, BH_3)	−25.5 (q, $^{1}J_{BH}$ = 80 Hz)
$[Cr(CO)_5(\eta^1\text{-}BH_2NMe_2BH_2NMe_2)]$ (**9a**)	1.84 (s, 12H, CH_3), −4.79 (q, $^{1}J_{BH}$ = 95 Hz, 2H, Cr−BH_2)[f]	4.7 (t, $^{1}J_{BH}$ = 118 Hz, noncoordinated BH_2), −2.4 (t,$^{1}J_{BH}$ = 95 Hz, Cr−BH_2)
$[W(CO)_5(\eta^1\text{-}BH_2NMe_2BH_2NMe_2)]$	1.81 (s, 12H, CH_3), −2.41 (q, $^{1}J_{BH}$ = 93 Hz, 2H, W−BH_2)[f]	4.6 (t, $^{1}J_{BH}$ = 114.7 Hz, noncoordinated BH_2), −6.6 (t, $^{1}J_{BH}$ = 93.1 Hz, W−BH_2)
$[Cr(CO)_5(\eta^1\text{-}BH_2N(CH_2)_4BH_2N(CH_2)_4)]$	2.44, 2.38 (m, 4H × 2, NCH_2), 1.30, 1.24 (m, 4H × 2, CH_2), −4.40 (br q, $^{1}J_{BH}$ = 100 Hz, 2H, Cr−BH_2)[f]	4.7 (t, $^{1}J_{BH}$ = 99 Hz, noncoordinated BH_2), −5.2 (t, $^{1}J_{BH}$ = 99 Hz, Cr−BH_2)
$[Cr(CO)_5(\eta^1\text{-}BH_2N(CH_2)_5BH_2N(CH_2)_5)]$	2.46, 2.18 (m, 4H × 2, NCH_2), 1.00, 0.69 (m, 6H × 2, CH_2), −4.63 (q, $^{1}J_{BH}$ = 95 Hz, 2H, Cr−BH_2)[f]	−0.3(t, $^{1}J_{BH}$ = 106 Hz, noncoordinated BH_2), −3.2 (t, $^{1}J_{BH}$ = 95 Hz, Cr−BH_2)
$[W(CO)_5(\eta^1\text{-}BH_2N(CH_2)_5BH_2(CH_2)_5)]$	2.46, 2.15 (m, 4H × 2, NCH_2), 1.01, 0.69 (m, 6H × 2, CH_2), −2.32 (q, $^{1}J_{BH}$ = 110 Hz, 2H, Cr−BH_2)[f]	−0.2 (br, noncoordinated BH_2), −7.2 (t, $^{1}J_{BH}$ = 110 Hz, W−BH_2)
$[Cr(CO)_5(\eta^1\text{-}BH_3\cdot NH_2Me)]$	1.47 (s, 3H, Me), −3.11 (br, 3H, BH)[g]	−17.7 (q, $^{1}J_{BH}$ = 98 Hz)
$[Cr(CO)_5(\eta^1\text{-}BH_3\cdot NH_2{}^tBu)]$	2.26 (br, 2H, NH_2), 0.49 (s, 9H, CH_3), −3.19 (q, br, 3H, $^{1}J_{BH}$ = 110 Hz, BH_3)	−27.4 (br)
$[W(CO)_5(\eta^1\text{-}BH_3\cdot NH_2{}^tBu)]$	2.20 (s br, 2H, NH_2), 0.47 (s, 9H, CH_3), −1.44 (q, 3H, $^{1}J_{BH}$ = 120 Hz, BH_3)	−32.2 (br)

[a] NMR spectra were recorded in benzene-d_6 at 500 MHz (^{1}H) or 160.4 MHz (^{11}B). [b] The NH resonance was too broad to be observed. [c] The other signals were overlapped with resonances of coupling products. [d] The methyne signal could not be detected because of the overlap with the methyne and BH resonances of free **1d**. [e] The cyclohexyl protons were not resolved because they overlapped with signals of other compounds in the reaction system. [f] The resonance of the terminal BH protons could not be observed because it was completely covered with the BH signals of free **2**. [g] The NH resonance was overlapped with that of the dehydrocoupling product, aminoborane oligomers.

photolysis and subsequent standing for 24 h at room temperature, the main product was $[BHNMe]_3$ (**5g**, 80%) as determined by NMR spectroscopy. In a similar manner, the dehydrocoupling reactions of various primary adducts were monitored in the presence of $[M(CO)_6]$ (5 mol %).[23c,d,28,30]

The photoreaction of $BH_3\cdot NH_2{}^tBu$ (**1i**) with equimolar $[W(CO)_6]$ provided a yellow solution, which showed NMR resonances assigned to $[W(CO)_5(\eta^1\text{-}BH_3\cdot NH_2{}^tBu)]$. Complexation of **1g** with chromium carbonyl was also confirmed. However, that of **1g** with tungsten carbonyl and coordination of **1h** to chromium or tungsten were not observed. The ^{1}H and ^{11}B NMR data of the borane complexes observed are given in Table 4.

Photoreaction of 1a with [Cr(CO)$_6$] in 1:1 Ratio. A C_6D_6 (0.5 mL) solution of **1a** (4.1 mg, 6.9×10^{-2} mmol) and $[Cr(CO)_6]$ (15.0 mg, 6.9×10^{-2} mmol) was prepared and sealed in a Pyrex NMR tube under high vacuum. The solution was photolyzed using a 450 W medium pressure Hg lamp. The ^{1}H and ^{11}B NMR spectra were recorded after 1, 5, and 20 min of photolysis. After that, the mixture was allowed to stand in the dark for 24 h at room temperature, and NMR spectra were recorded.

Computational Details. Stationary points were located by density functional theory (DFT) using a hybrid functional PBE0, which is also referred to as PBE1PBE.[51] Chromium was described with the effective core potentials (ECP) of Hay and Wadt with a double-ζ valence basis set (LANL2DZ)[71] augmented with f-polarization functions (α = 1.941).[72] A double-ζ plus polarization valence basis set augmented with diffuse functions, 6-31++G(d,p) was employed for B, N, and BH and NH hydrogen atoms, which directly participated in the dehydrocoupling. For all other atoms, a standard 6-31G(d) basis set was applied. Geometry optimizations were also conducted using several types of functionals for some species. The structures given by the B3PW91,[73,74] mPW1PW91,[75] MPW1K,[76] and PBEPBE[51] functionals were essentially the same as that of PBE0 except for very slight differences in bond distances and angles. However, the B3LYP[73,77] structure of **3a** differed substantially from the PBE0 geometry.[78] Vibration analyses were then performed at the same level of theory (PBE0) to characterize

(71) (a) Hay, P. J.; Wadt, W. R. *J. Chem. Phys.* **1985**, *82*, 270. (b) Wadt, W. R.; Hay, P. J. *J. Chem. Phys.* **1985**, *82*, 284. (c) Hay, P. J.; Wadt, W. R. *J. Chem. Phys.* **1985**, *82*, 299.
(72) Ehlers, A. W.; Böhme, M.; Dapprich, S.; Gobbi, A.; Höllwarth, A.; Jonas, V.; Köhler, K. F.; Stegmann, R.; Veldkamp, A.; Frenking, G. *Chem. Phys. Lett.* **1993**, *208*, 111.
(73) Becke, A. D. *J. Chem. Phys.* **1993**, *98*, 5648.
(74) Perdew, J. P.; Wang, Y. *Phys. Rev. B* **1992**, *45*, 13244.
(75) Adamo, C.; Barone, V. *J. Chem. Phys.* **1998**, *108*, 664.

the stationary points and to determine thermochemical parameters including entropies. The connectivity of important transition states was confirmed by performing intrinsic reaction coordinate (IRC) calculations.[79,80]

The single point energies were then calculated with the DFT/PBE0 level of theory. At this stage, Stuttgart−Dresden ECP and valence triple-ζ plus f-polarization basis set (SDD) were used for chromium,[81] and Dunning's double-ζ class basis set augmented with polarization and diffuse functions, aug-cc-pVDZ, was employed to describe the other atoms.[82] In addition, the CPCM model[52] was applied to estimate the energies in solution. To the solvation free energies thus obtained, the Gibbs free energy contributions, which were given in the vibration analyses, were added to consider the entropic terms. The values of the solvation free energies are given as those at 298 K and 1 atm in benzene. BSSE corrections were not performed. All calculations were performed with the Gaussian 03 package of programs.[83]

Acknowledgment. This work was supported by Grant-in-Aid for Scientific Research on Priority Areas (No. 14078101, "Reaction Control of Dynamic Complexes") from Ministry of Education, Culture, Sports, Science and Technology, Japan. We are grateful to Professor Sakaki of Kyoto University for his kind suggestion in the computational study. We thank Professor Koe of International Christian University for the help of preparation of the manuscript.

Supporting Information Available: The Cartesian coordinates, electronic energies, and Gibbs free energies of all the optimized structures, the ^{11}B spectral change during the Cr-catalyzed dehydrocoupling of **1g**, and complete ref 83. This material is available free of charge via the Internet at http://pubs.acs.org.

JA904918U

(76) (a) Lynch, B. J.; Fast, P. L.; Harris, M.; Truhlar, D. G. *J. Phys. Chem. A* **2000**, *104*, 4811. (b) Lynch, B. J.; Truhlar, D. G. *J. Phys. Chem. A* **2001**, *105*, 2936.
(77) Lee, C. T.; Yang, W. T.; Parr, R. G. *Phys. Rev. B* **1988**, *37*, 785.
(78) In the B3LYP-optimized structure of **3a**, the NH proton of the BH_3·$NHMe_2$ ligand interacted with a carbonyl oxygen atom instead of the chromium center.
(79) Fukui, K. *Acc. Chem. Res.* **1981**, *14*, 363.
(80) (a) Gonzalez, C.; Schlegel, H. B. *J. Chem. Phys.* **1989**, *90*, 2154. (b) Gonzalez, C.; Schlegel, H. B. *J. Phys. Chem.* **1990**, *94*, 5523.
(81) (a) Häussermann, U.; Dolg, M.; Stoll, H.; Preuss, H.; Schwerdtfeger, P.; Pitzer, R. M. *Mol. Phys.* **1993**, *78*, 1211. (b) Kuechle, W.; Dolg, M.; Stoll, H.; Preuss, H. *J. Chem. Phys.* **1994**, *100*, 7535. (c) Leininger, T.; Nicklass, A.; Stoll, H.; Dolg, M.; Schwerdtfeger, P. *J. Chem. Phys.* **1996**, *105*, 1052.
(82) Dunning, T. H., Jr. *J. Chem. Phys.* **1989**, *90*, 1007.
(83) Frisch, M. J.; et al. *Gaussian 03*, Revision D.01; Gaussian, Inc.: Wallingford CT, 2004.